U.S. Department
of Transportation
**Federal Railroad
Administration**

Improved Source Location Using Sensor Arrays

**Office of Research and
Development
Washington, D.C. 20590**

DOT\FRA\ORD\98\05 **June 1998**

DISCLAIMER

This document is disseminated under the sponsorship of the Department of Transportation in the interest of information exchange. The United States Government assumes no liability for the contents or use thereof. The United States Government does not endorse products or manufacturers. Trade or manufacturers' names appear herein solely because they are considered essential to the object of this report.

Technical Report Documentation Page

1. Report No.	2. Government Accession No.	3. Recipient's Catalog No.
FRA/ORD/98/05		

4. Title and Subtitle	5. Report Date
Improved Source Location Using Sensor Arrays	June 1998
	6. Performing Organizational Code: Cyltek, Inc
7. Author(s): Mark P. Connolly and James Lyman	8. Performing Organization Report No.
9. Performing Organization Name and Address: Cyltek, Inc. 310A Breesport San Antonio, Tx 78216	10. Work Unit No. (TRAIS)
	11. Contract or Grant No.: DTRS57-97-C-00077
12. Sponsoring Agency Name and Address: Federal Railroad Administration 400 7th Street SW Washington, DC 20590	13. Type of Report and Period Covered: Final (10/97-6/98)
	14. Sponsoring Agency Code: FRA

15. Supplementary Notes

16. Abstract

The purpose of this research was to develop a sensor array capable of identifying the location of acoustic sources. The sensor array was constructed from a polymer known as PVDF. The array was created using an etching technique similar to that used for printed circuit boards. An amplifier was designed and built for this array. A microprocessor controlled digital logic board was built that was capable of analyzing the output from up to 16 pre-amplifiers. The logic board was capable of analyzing the output from a 4 by 4 sensor array as an acoustic wave traversed the sensor elements. A number of trials with the sensor-array and associated electronics showed that it was capable of identifying the direction of a number of sources.

17. Key Words	18. Distribution Statement
Acoustic emission, location sensor-array.	

19. Security Classif. (of this report)	20. Security Classif. (of this page)	21. No. of Pages	22. Price
		46	

Table of Contents

List of Figures

List of Tables

1.0 Executive Summary

Purpose of the Research: The purpose of the research was to develop a sensor array capable of identifying the location of acoustic sources. Accurate source location enables critical defects such as cracks to be identified during acoustic emission inspection of rail tank cars. This is not possible with current acoustic emission sensor technology.

Description of the research: The sensor array was constructed from a piezo-electric polymer film known as Polyvinylidene Flouride (PVDF). The polymer-film was chosen since, unlike conventional ceramic sensors, it can be etched into sensor arrays using a process very similar to that used for printed circuit board fabrication. A number of sensor arrays were constructed for testing.

The sensitivity of the polymer film is significantly less than that of the ceramic, therefore a novel positive feedback circuit was designed to provide very high amplification with low noise. An extensive study was performed to select the optimum amplifier chip for this circuit, and was used together with a band-pass filter to reduce low and high frequency noise. Extensive benchmark comparisons were performed using a commercial ceramic sensor. The results show that the output from the polymer-film sensor and pre-amplifier was typically only 8 dB lower than that of the commercial resonance type ceramic sensor.

A microprocessor controlled digital logic board that was capable of analyzing the sensor output from up to 16 pre-amplifiers was designed and built. This board was capable of processing the output from a 4 by 4 sensor array by producing a memory image of the sensor array as the wave traversed the sensor elements. The logic board was also capable of buffering this data through an RS-232 to a computer.

Results: A number of trials were performed with the sensor-array, pre-amplifiers and logic boards. The system was connected through the RS-232 to a computer and a number of trials were performed using sound sources at known locations. In all cases the sensor was capable of identifying the angular location of the source.

Recommendations: Further work with the sensor-array should focus on minimizing the size of the array elements and associated electronics. The electronics should also be mounted above the sensor array to further reduce the size of the unit. Extensive trials should then be performed with this sensor-array on actual tank cars. This will provide the validation data required for acceptance in the standards.

Potential applications of the research: The research performed here represents a major advance in sensor technology for acoustic emission. Location has rarely been used for source discrimination due to inaccuracies with conventional acoustic emission location techniques based on the arrival time of the signal at a sensor. An acoustic emission sensor array was shown to be capable of locating the sources. This approach would fundamentally alter acoustic emission inspection since it would enable the sources to be accurately and unambiguously located. For example cracks in rail tank cars could be easily

distinguished from less significant corrosion or from noise, a process that is not feasible with current technology. This sensor also could be used for many other applications such as ultrasonics or medical imaging.

2.0 Introduction

Acoustic emission (AE) is a test technique that is used in place of the hydrostatic test for rail tank car inspection. Acoustic emission involves placing sensors on the tank car and measuring the acoustic activity as the car is stressed. Defects will normally emit acoustic events that radiate as sound waves from the source to the sensors. The critical defects are often cracks and for these defects to be clearly identified source location is needed. The acoustic activity from cracking will appear on the source location map as a tight cluster of acoustic events, allowing for easy identification.

As an example of the benefit of this approach consider the results from an AE inspection of a high pressure steel cylinder shown in Figure 1. The rectangular region in the figure represents an unfolding of the cylinder sidewall and the circles represent the hemispherical ends. A cluster of emissions is circled. These emissions were detected and located using source location. A follow-up metallurgical examination indicated that this cluster of emissions was produced by the fatigue crack shown in the figure.

Source location worked well for this case primarily due to the simple geometry of the cylinder. Conventional source location is based on the concept of time-of-arrival. By determining the arrival time at three sensors the location of the source can be determined by triangulation and this is shown in Figure 2. The velocity of sound is required to convert the arrival time to the distance traveled.

The time-of-arrival is determined when the signal exceeds a threshold. The approach can produce large errors since the time-of-arrival is dependent on the threshold level selected. Secondly acoustic emission signals are often multi-modal; a single value of the velocity does not represent all of the wave modes and will produce erroneous locations.

To overcome these shortcomings an alternative approach was proposed using a sensor-array to determine the direction of the wave-front. The singular advantage of this approach is that the sensor array can provide a direction vector, therefore it does not employ time-of-arrival. A schematic diagram of the sensor array approach is shown in Figure 3. By knowing the direction of the wave-front at two sensors it will be possible to determine the location of the source as the intersection of the vectors.

The major challenge is to develop a sensor array that is capable of locating the acoustic emission sources in practical applications and that can be produced at a reasonable cost.

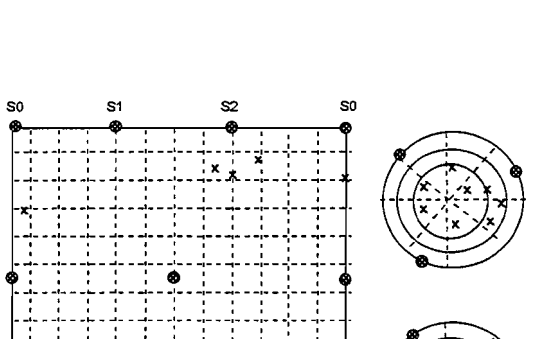

(a)

(b)

Figure 1: Source location map (a) of a high pressure gas cylinder, the circled region represents the emission from a crack. A follow-up metallurgical examination (b) identified a crack at this location.

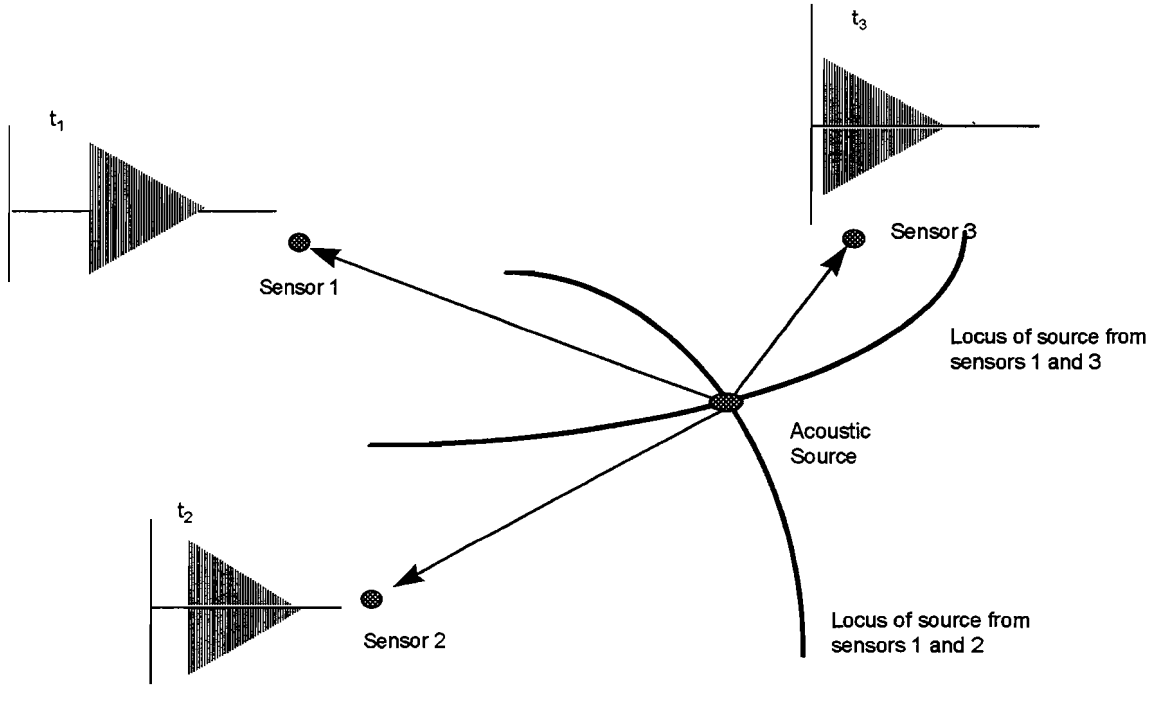

Figure 2. Schematic diagram showing triangulation of arrival times to determine the source of the acoustic emission signal.

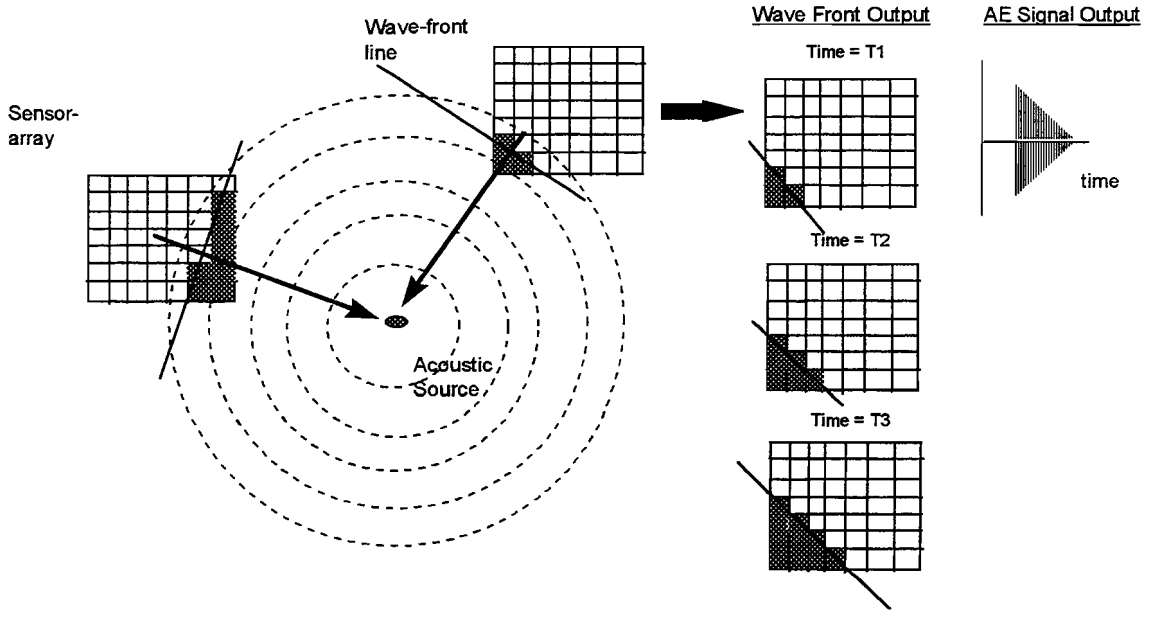

Figure 3. Schematic diagram of the sensor-array used for source location. The primary output from the sensor-array is the direction of the wave-front.

2.1 Background to PVDF Polymer-Film Sensors

Sensors for AE inspection are primarily made from lead zirconate titanate (PZT) ceramics. PZT is the material of choice since it has a high sound efficiency, that is, it produces a large electrical output for a given sensor displacement. However PZT cannot be used for sensor arrays since the ceramics must be saw-cut. An alternative approach is to use piezoelectric polymer films such as Polyvinylidene Flouride (PVDF). PVDF is a flexible film that can be etched and therefore used as a sensor array.

The properties of PVDF include:

(1) Wide frequency range (1 Hz to 10^9 Hz)
(2) Large dynamic range (10^{-8} to 10^6 psi)
(3) Low acoustic impedance (close match to water)
(4) High elastic compliance
(5) Ease of manufacture

Although the low acoustic impedance provides a good match for human tissue this is less significant for metals. The sensors are also sensitive to electromagnetic radiation and good shielding techniques are required.

PVDF has been used by a number of researchers to make sensor-arrays. Some of this work has been performed for medical imaging where the primary objective has been to develop systems for ultrasonic computed tomography. For example Filling et al[1] developed a 46 element PVDF sensor-array and showed marked improvements over a PZT sensor in reducing artifacts associated with ultrasonic imaging.

PVDF arrays have been used either as a range sensor[2] or as a tactile sensor placed on a robotic gripper[3]. For example the US Air Force developed a tactile sensor for robotic applications using a PVDF array. A silicon integrated circuit was designed for a 5 by 5 matrix array on an 8 mm square element. The primary difficulty of the sensor-array is the data handling cost associated with large numbers of sensor elements. Therefore novel instrumentation is required to produce a sensor-array that can be used in practical applications and that can be produced at a reasonable cost.

---

[1] Dale W. Fitting, Paul L. Carson, Jeffrey J. Giesey and Patrick M. Grounds., "A Two-Dimensional Array Receiver for Reducing Refraction Artifacts in Ultrasonic Computed Tomography of Attenuation" IEEE Transactions on Ultrasonics, Ferroelectrics and Frequency Control, Vol. UFFC-34, No. 3, May 1987
[2] Antonio S. Fiorillo, "Design and Characterization of a PVDF Ultrasonic Range Sensor" IEEE Transactions on Ultrasonics, Ferroelectrics and Frequency Control, Vol. 39, No. 6, Nov 1992
[3] Kolesar E. S., Reston R. R., Ford D. G and Fitch R. C., "Object Imaging with a Multiplexed Piezoelectric Polymer Tactile Sensor" IEEE 1991.

3.0 Development of Prototype Sensor Array

3.1 Procurement of PVDF Film

PVDF polymer-film was procured from AMP[4] a manufacturer of PVDF film. Two types of film were selected and these are given in Table 1. A schematic diagram of the film is shown in Figure 4. The polymer films were metallized for easy attachment of electrical leads. A photograph of the PVDF sheet (taken from the AMP catalog) is shown in Figure 5.

Table 1. List of PVDF film selected

Part No	Thickness (μm)	Metallization	Film Size
1-1004347-0	28	Silver Ink	203 mm by 127 mm
3-1004346-0	110	Silver Ink	203 mm by 127 mm

3.2 Sensor Amplification

PVDF polymer-film sensors have relatively poor sensitivity when compared with ceramic PZT sensors. For example, under real-world conditions the output from a PZT ceramic will be orders of magnitude higher than that of a PVDF film sensor. Therefore careful amplification is required. Two pre-amplifier designs were considered. The first uses a conventional voltage amplifier and the second used positive feedback. For each of these designs a range of commercial amplifiers with very good gain-bandwidth characteristics and low noise were evaluated. Each design is considered in turn.

A schematic diagram of the straight voltage amplifier design is shown in Figure 6. Seven quad, low noise, high speed amplifier chips were evaluated as the op-amps for this circuit and these are listed in Table 2. Two of the amplifiers, TL074 and LT1114 had poorer gain/bandwidth product but were included for comparison.

Table 2. List of Candidate Amplifiers Tested

Amplifier Type	Manufacturer
LT1125	Linear Technology
LT1356	Linear Technology
MAX414	Maxim
LT1365	Linear Technology
LT1114	Linear Technology
LT1359	Linear Technology
TL074	Texas Instruments

[4] Amp Incorporated, PO Box 799, Valley Forge, PA 19482-0799

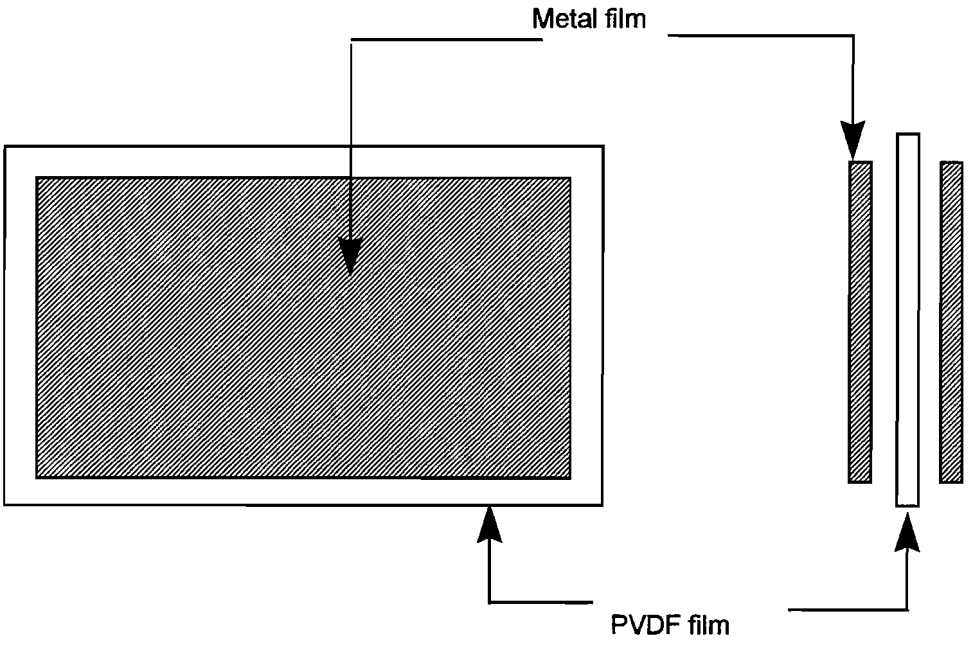

Figure 4. Schematic diagram of the PVDF polymer-film sensor.

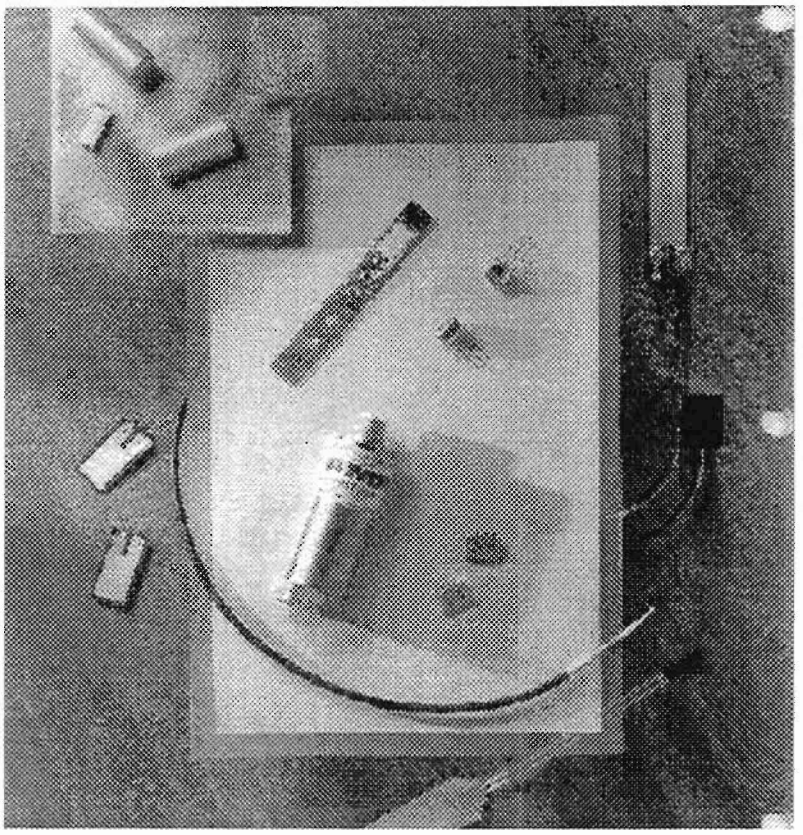

Figure 5. Photograph of the PVDF polymer-film taken from the Amp catalog. Also shown are smaller objects that use the PVDF film.

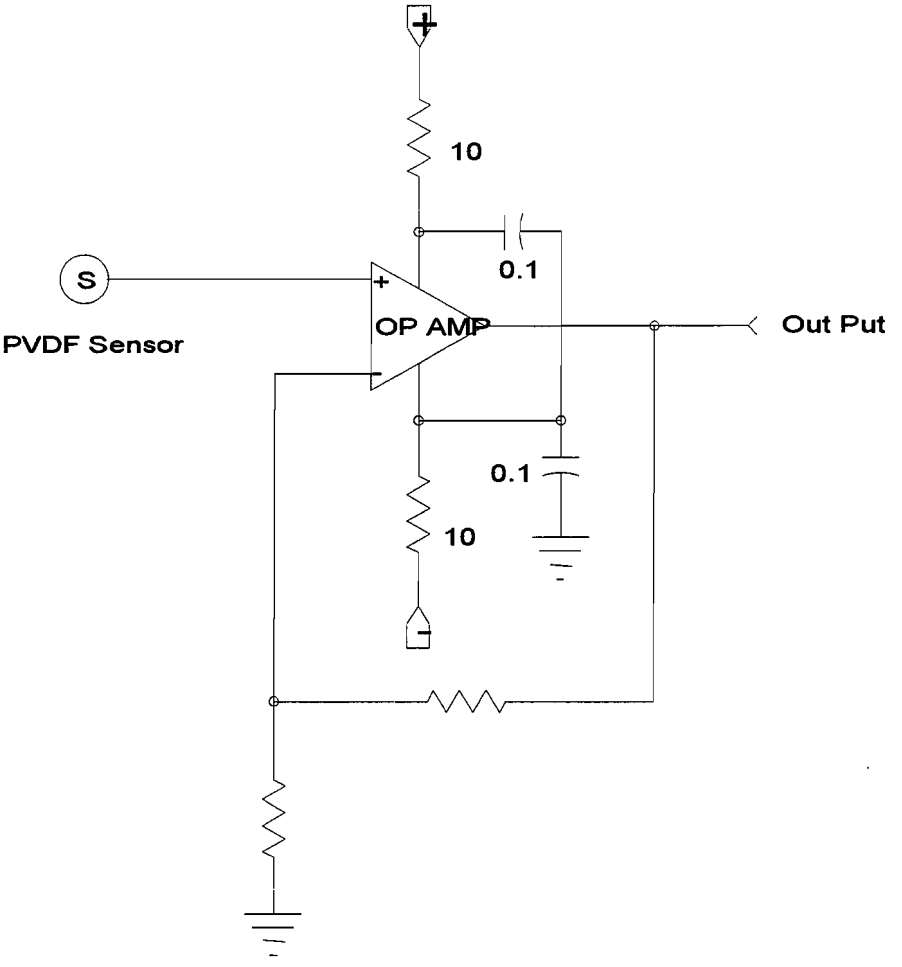

Figure 6. Circuit diagram for voltage amplifier.

Each of the amplifiers were used in the circuit shown in Figure 6 and the gain and noise characteristics were determined in order to select the best amplifier for this application. The resistor values were chosen to provide the maximum gain for each of the amplifiers at the frequency of 150 kHz. A summary of each of the amplifier characteristics optimized for 150 kHz is given in Table 3.

Table 3. Summary of Amplifier Characteristics

Amplifier Type	Max. Available Gain at 150 kHz	Specified Noise nV/√f	Input Impedance (Mohms)
LT1125	35	3	1
LT1356	30	10	160
MAX414	69	2.4	40
LT1365	174	9	50
LT1114	1.9	16	700000
LT1359	60	8	80
TL074	9.1	18	1×10^{12}

In order to determine the gain and noise characteristics of the amplifiers, tests were performed using simulated acoustic emission sources. The test setup is shown in Figure 7.

In Figure 7 the PVDF polymer sensor was placed on a metal plate. A small pulser was used as a simulated source. A commercial resonance type PZT sensor (R15I manufactured by Physical Acoustics Corporation) was placed adjacent to the PVDF sensor. A photograph of the test setup is shown in Figure 8. Circuit boards were built for each of the amplifiers as shown in Figure 9. The results from these tests are given in Table 4.

Table 4. Results from Simulated Tests for Voltage Amplifier

Amplifier Type	Noise with sensor floating (dB)	Noise with sensor on plate (dB)	AE signal mV pp
LT1125	35	3	10
LT1356	30	10	10
MAX414	69	2.4	0
LT1365	174	9	0.3
LT1114	1.9	16	0.5
LT1359	60	8	0
TL074	9.1	18	3.6

The results in Table 4 require some explanation. The noise columns in the table represent the difference between the case where the amplifier was not powered and the case where

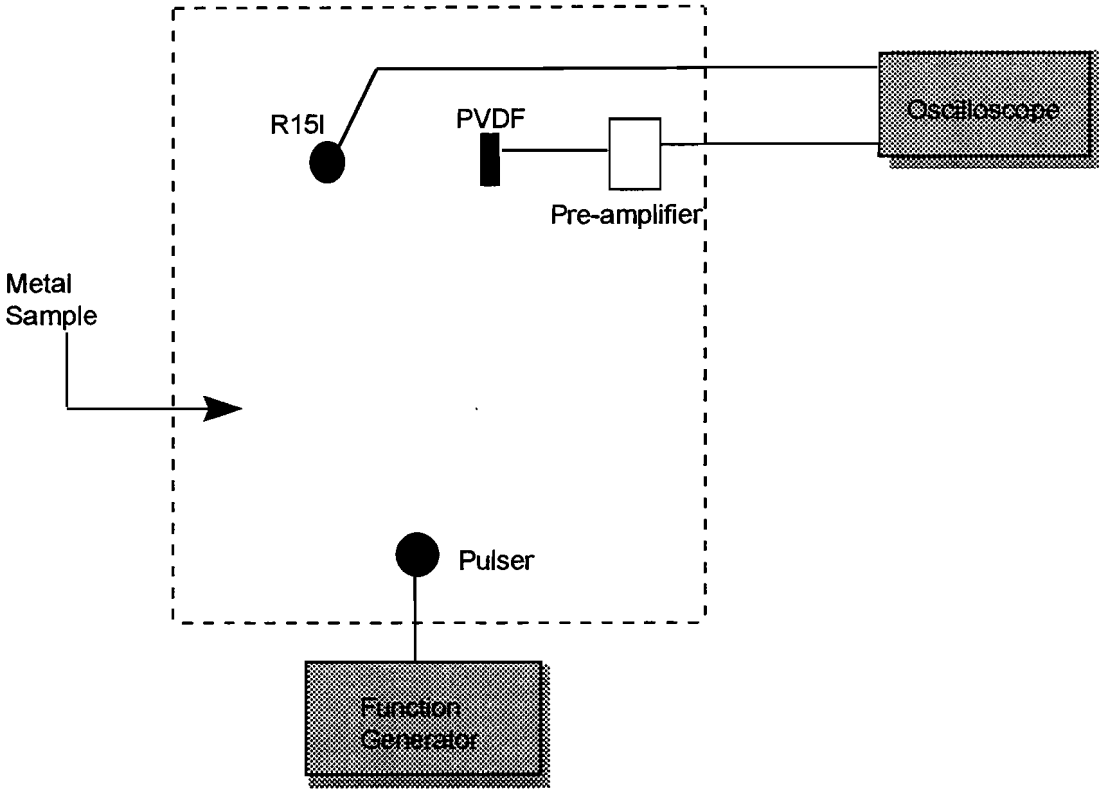

Figure 7. Schematic diagram of the experimental setup used to determine the performance of the amplifier.

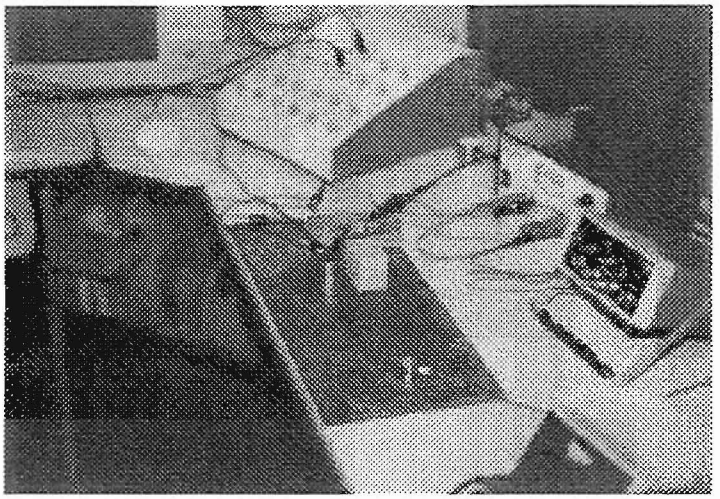

Figure 8. Photograph of the test setup used to evaluate the performance of the pre-amplifiers.

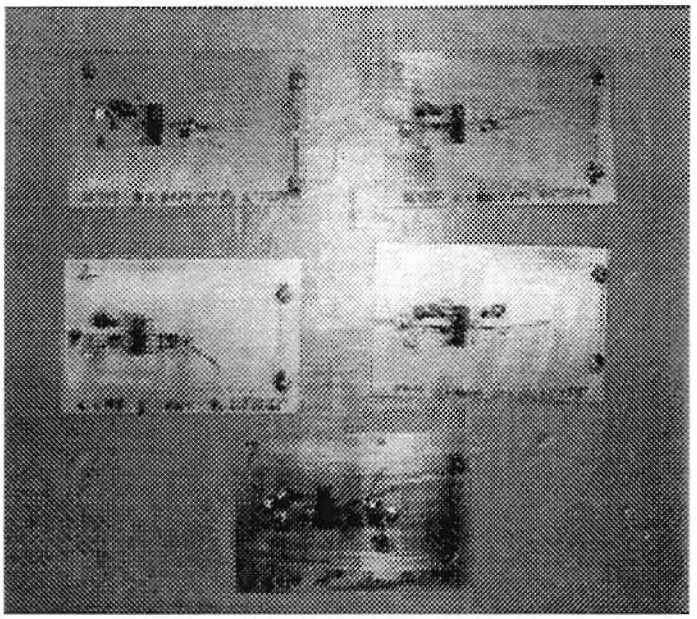

Figure 9. Photograph of some of the trial pre-amplifiers.

the amplifier was turned on. For the case where the amplifier was not powered and the sensor was floating, large signals were obtained as a result of the sensor acting as an antennae. This was a feature of the PVDF sensor which was sensitive to RF interference. The final column represents the voltage output and is the most important number. For some of the amplifier designs no measurable signal was obtained. Table 4 also shows that the maximum signal obtained, after amplification, was reasonably small. Considering that the source was strong and near the sensor these signals are unacceptable. For example, for the conventional R15I sensor, which is fabricated from ceramic PZT, a signal of 1000 mV was obtained, a factor of 100 greater than the best case results given in Table 4.

An alternative amplifier design, known as a charge amplifier, with positive feedback, was used. In this design the amplification occurs directly with the current and this circuit can more properly be called a voltage converter. The circuit diagram is shown in Figure 10. In this circuit positive feedback was used. Positive feedback is very old but little used method because of the strong tendency for the amplifier to oscillate. By careful control of the feedback, amplification in excess of times 1000 was achievable. The tests performed for the voltage amplifier were repeated and the results are given in Table 5.

Table 5. Results from Simulated Tests for Charge Amplifier

Amplifier Type	AE signal mV pp	Resistance Kohm
LT1125	260	98
LT1356	80	140
MAX414	140	242
LT1365	150	360
LT1114	3	50
LT1359	100	211
TL074	20	26

For the charge amplifier design the feedback resistance changes the gain. The resistance was selected to provide the maximum gain and these are the values given in the table. The results in the table show that amplifier LT1125 provided the maximum output. The sensor output for the R15I sensor was typically in the range of 1000 mV and therefore these results compare reasonably well with this sensor. Although the above results show that excellent response was obtained using the LT1125 one of the problems with the charge amplifier design is that it is frequency sensitive. The resistance values given in Table 3 was optimized for 150 kHz and the gain will be less as the frequency deviates from this value.

For this amplifier design the effects of feedback capacitance and resistance on the amplifier output were studied. Figure 11 shows the effects of the feedback capacitance and the very large increase in amplification with decreasing feedback. Figure 11 shows that with very small capacitance very large outputs were obtained. This test was performed with the 110 μm polymer film. However with very small capacitances the circuit tends to be very unstable and is susceptible to oscillators as a result of random noise. Therefore a

capacitance of 2 pF was used since it appears to provide a good compromise between high gain and a stable output. The effects of feedback resistance was also studied and this result is shown in Figure 12. Figure 12 shows that for the 2 pF capacitance the gain is reasonably stable over a wide resistance range.

3.3 Performance of Sensor/Pre-Amplifier.

The above results show that excellent response was obtained using the LT1125 amplifier. However the amplifier design uses positive feedback which can be very sensitive to amplifier-to-amplifier lot variations. In order to determine if this variation was significant tests were performed on 16 LT1125 amplifiers. The tests were also designed to comprehensively compare the performance of the PVDF sensor/pre-amplifiers with a commercial resonance type PZT sensor (R15I manufactured by Physical Acoustic Corp.)

The tests were performed in manner similar to that shown in Figure 7. Two metal samples were used for testing, a thin aluminum sheet (1.6 mm thick) and a thicker steel sheet (4.7 mm thick). The output from both sensors were monitored with a high speed A/D board on a PC computer and the wave-forms were stored for later analysis.

A typical example of the wave-forms obtained from both sensors is shown in Figure 13. As shown in Figure 13 the response of both sensors was similar however the output from the PVDF polymer-film sensor was lower than that of the PZT ceramic sensor, although this sensor has an integral 40 dB pre-amplifier. From Figure 13, for the PZT sensor the peak to peak was approximately 10 V whereas for the PVDF polymer-film sensor the peak to peak was 300 mV, which represents a 30 dB difference.

Figure 13 also shows that the noise from the PVDF polymer-film sensor is substantially higher than that from the PZT ceramic sensor. This is clear from the trace where the signal has decayed.

The tests were repeated for 16 separate LT1125 amplifiers and with the two metal sheets and the results are given in Table 6. The ratio of the peak to peak voltages were calculated for the PZT and the PVDF sensors and these results are given in the table. These ratios are also expressed in dB. The average difference between the PZT and the PVDF sensor was 29.1 dB for the aluminum plate and 27.5 dB for the steel plate. In view of the lower amplitude signal for the PVDF sensor, extra gain was applied to the circuit. To reduce the noise a band-pass filter was also added to the output from the pre-amplifier.

A diagram of the full pre-amplifier circuit is shown in Figure 14. The output from the pre-amplifier was applied to the input of a high pass active filter, whose cut-off frequency was about 18 KHz. Because of the upper frequency roll off the filter is actually a band pass filter with a cut-off frequency of 250 KHz. This band pass filter further reduces both the low and high frequency noise. This filter also has a voltage gain of about ten, further increasing the signal's voltage output level, while maintaining the same signal to noise ratio.

Table 6. Comparison between output of PVDF polymer-film sensor with pre-amplifier and R15I sensor (PZT).

Amplifier ID	PZT/PVDF (Al sheet)	PZT/PVDF (dB) (Al sheet)	PZT/PVDF (Steel sheet)	PZT/PVDF (dB) (Steel sheet)
1	0.0435	-27.2	0.0465	-26.7
2	0.0342	-29.3	0.0397	-28.0
3	0.0487	-26.3	0.0349	-29.1
4	0.0481	-26.3	0.0320	-29.9
5	0.0432	-27.3	0.0461	-26.7
6	0.0370	-28.6	0.0465	-26.6
7	0.0405	-27.8	0.0460	-26.7
8	0.0365	-28.8	0.0446	-27.0
9	0.0328	-29.7	0.0381	-28.4
10	0.0334	-29.5	0.0529	-25.5
11	0.0339	-29.4	0.0537	-25.4
12	0.0343	-29.3	0.0446	-27.0
13	0.0313	-30.1	0.0345	-29.2
14	0.0254	-31.9	0.0340	-29.4
15	0.0310	-30.2	0.0403	-27.9
16	0.0211	-33.5	0.0444	-27.0

As shown in Figure 14 the output from the band-pass filter was input to the a simple AC coupled voltage amplifier, with an upper cut off frequency of 350 KHz. The output from the pre-amplifier with filters and extra gain produces an output similar to that of the R15I sensor. The circuit shown in Figure 14 consisting of the pre-amplifier, the band-pass filter and the extra gain is known generically as a pre-amplifier. Four pre-amplifiers were mounted on brass boards since the LT1125 chip is in the form of a quad chip. A brass board pre-amplifier is shown in Figure 15.

3.4 Sensor Anisotropy

The response of the sensor as a function of angular location was determined by changing the source from 0 to 45 to 90 degrees. The results from these tests are given in Table 7. Table 7 shows that the response for the PZT sensor is relatively constant whereas the response of the PVDF sensor changes. However there does not seem to be a systematic trend. In fact observations during testing showed that the response of the PVDF sensor was very sensitive to the sensor mounting and that the sensors had to be placed carefully on the specimen in order to obtain acceptable results.

Table 7. Effect of Source Orientation on Signal Amplitude

Plate Thickness (in)	Angle (deg)	PZT (mvPP)	PVDF (mvPP)
3/16	0	3.04	152
3/16	45	2.83	132
3/16	90	2.95	85
0.062	0	0.836	226
0.062	45	0.836	184
0.062	90	0.836	256

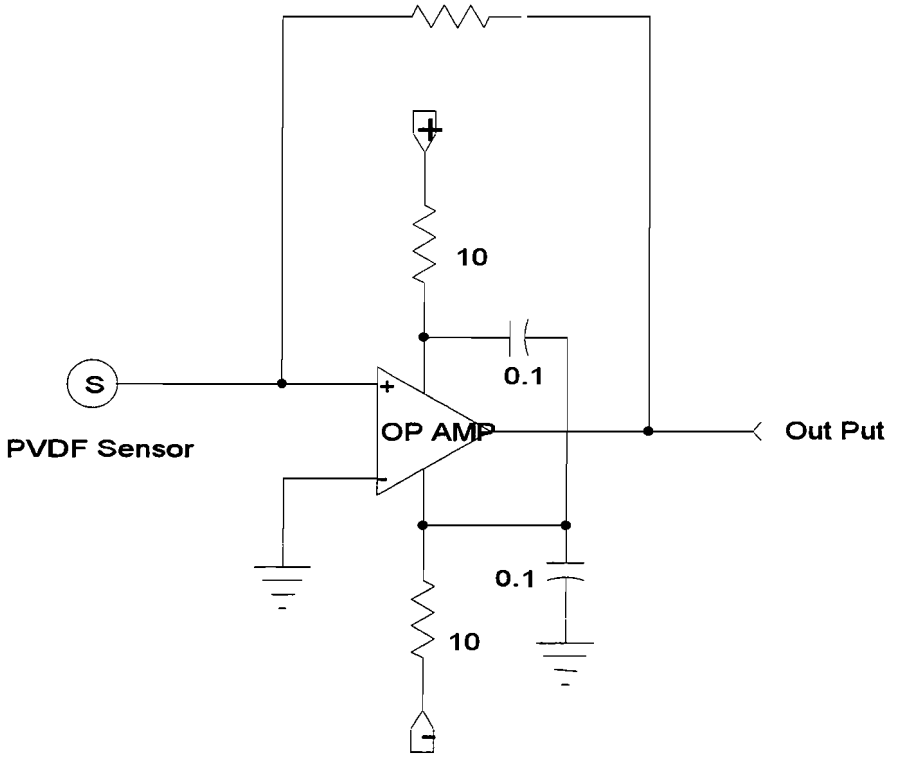

Figure 10. Circuit diagram for charge amplifier with positive feedback.

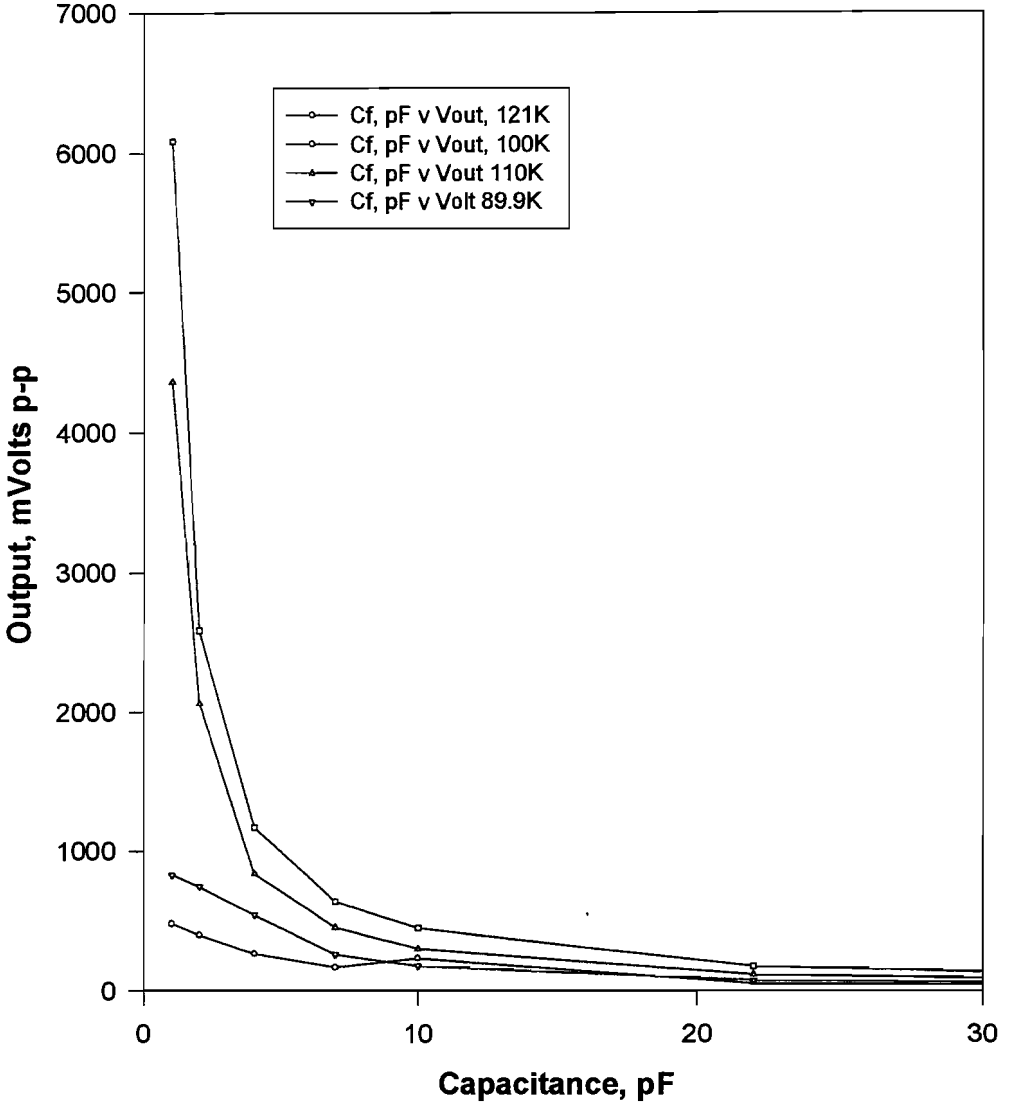

Figure 11. Effect of feedback capacitance on the amplifier output.

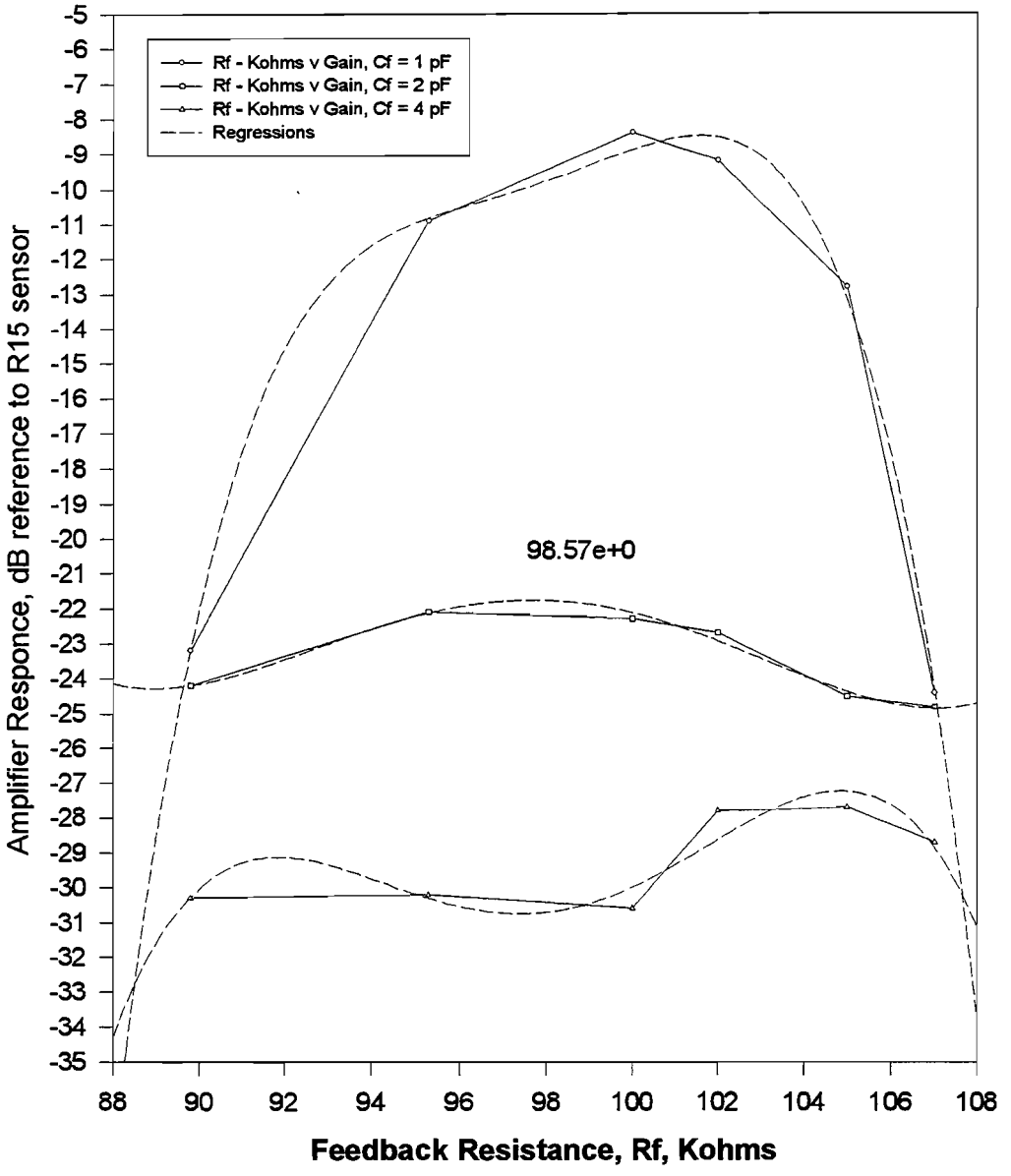

Figure 12. Effect of feedback resistance on the amplifier output.

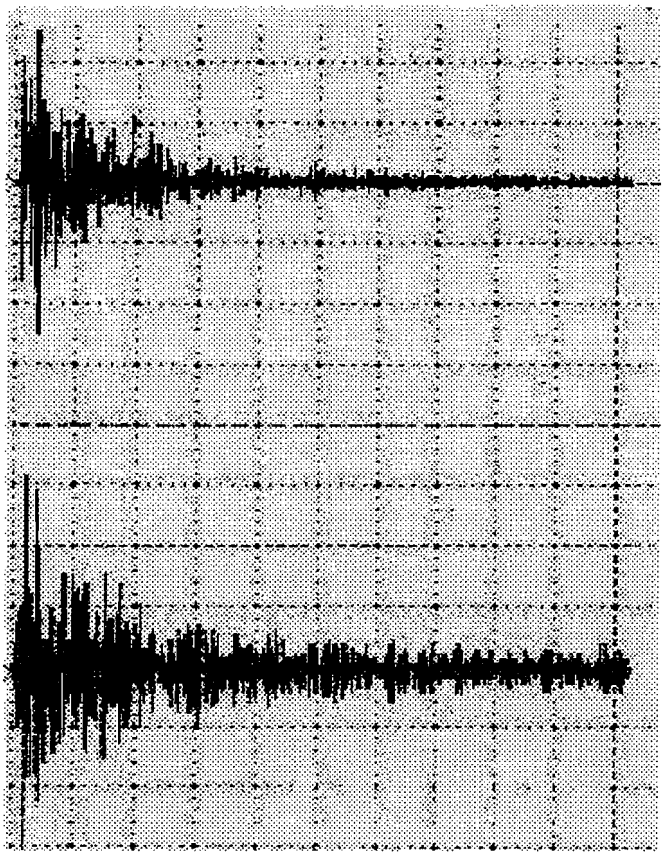

Figure 13. Typical comparison between R-15I sensor (top) and PVDF polymer-film sensor (bottom). The scale for the R-15I sensor is 2V/d and for the PVDF polymer-film is 50 mV/d.

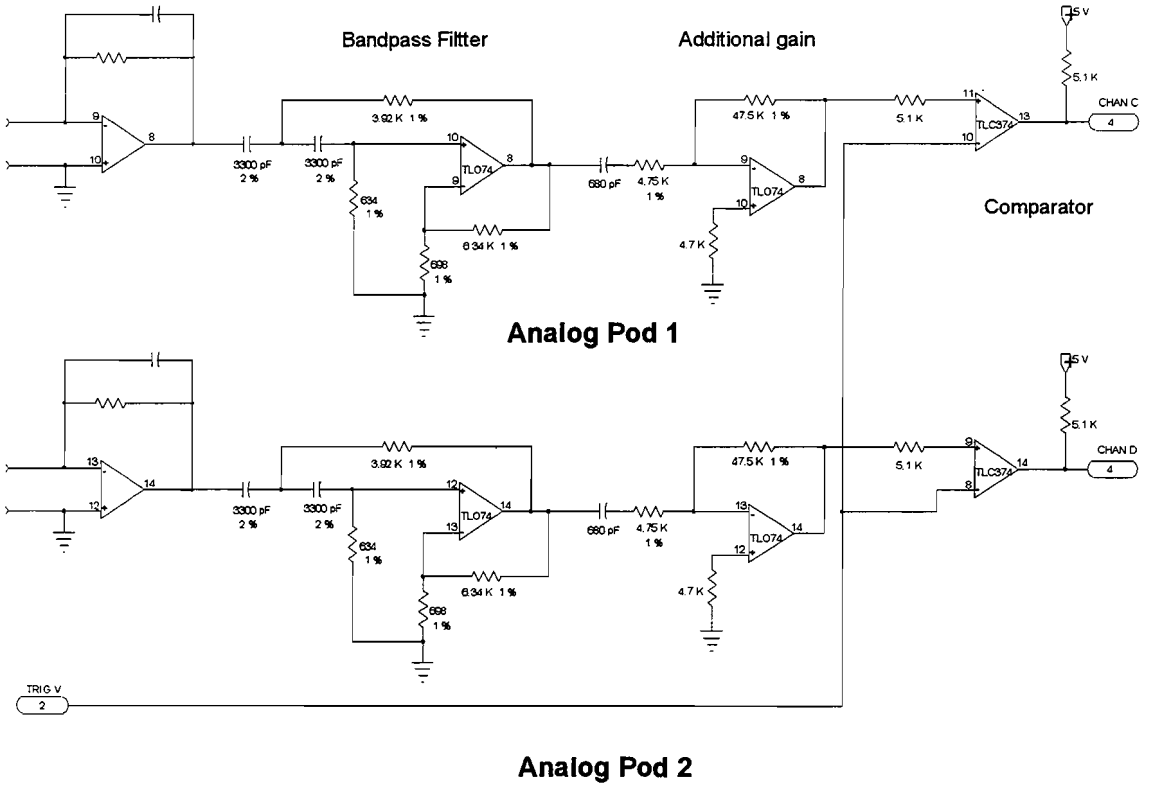

Figure 14. Circuit diagram for analog pod showing pre-amplifier, band-pass filter and extra gain. Two analog pods are shown in the figure.

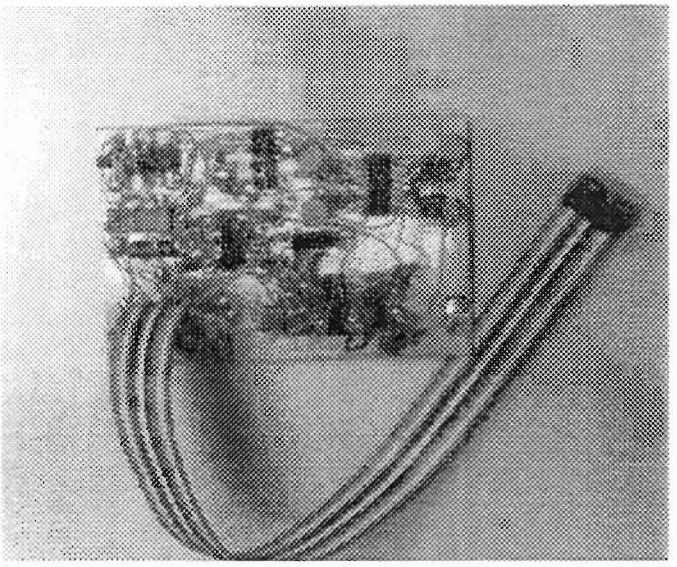

Figure 15. Photograph of the pre-amplifier board. Each brass board consists of four pre-amplifiers.

4.0 Overall System Design

Section 3.0 described the design of the sensor pre-amplifier stage. These pre-amplifiers were incorporated into an overall system design that was capable of determining the direction of the wave-fronts. Prior to describing the electronic hardware the overall approach is described.

To determine the direction of the wave-front the approach shown schematically in Figure 16 was followed. An image is kept in memory that is a mirror of each location in the sensor array. Each memory location is connected to each sensor element through the associated electronics. As the wave-front passes under the sensor it sets the corresponding location in memory to high if the voltage level exceeds a fixed threshold. This process continues and the memory location are successfully filled up as the wave-front traverses across the sensor as shown in the figure.

The purpose of the electronic design is to realize Figure 16. The overall system design is shown in Figure 17 and in Figure 18. In Figure 17 the fully amplified and filtered acoustic signal from each of four pre-amplifiers, corresponding to a row in a 4 by 4 sensor array is input to a comparator. Figure 17 is referred to as an analog pod and as shown in Figure 17 each analog pod can analyze the output from four sensors. A DC reference voltage that represents the signal threshold voltage is continuously compared with the incoming AC signal from each of the sensors and if the positive swing exceeds the threshold voltage, the output goes to a TTL high. The DC threshold voltage is set manually via a multi-turn potentiometer.

The TTL outputs of each of the four camparators is applied to an RS latch, whose output is set initially to a TTL low state, but goes to and remains at a TTL high when the output of the comparator first goes high. The output from the TTL latch is applied to a OR logic network, such that a TTL high occurs anytime one or more of it's input goes high. This generates a trigger signal which indicates one of the sensor elements signal has exceeded the threshold level. The trigger signal is applied to the control logic to start the writing of data to RAM.

The logic board block diagram is shown in Figure 18 and a photograph of the logic board is shown in Figure 19. In Figure 18 the output from the analog pod is input to the trigger OR which causes a latch to be set. A memory address is generated by a clock gate and the data is written to the RAM memory using a multiplexer. The multiplexer is needed since the data from the RAM must be read from and written to, and this is controlled by the multiplexer. A CMOS 6116 was used as RAM. When the RAM was full a microprocessor (8051) read the data from the RAM and send it to the RS-232 where it was read by a computer. In order to be able to read the RAM memory and send it to the RS-232 the analog POD's were turned off. At the completion of a read cycle the microprocessor reset all of the latches on both the analog pods and the logic boards.

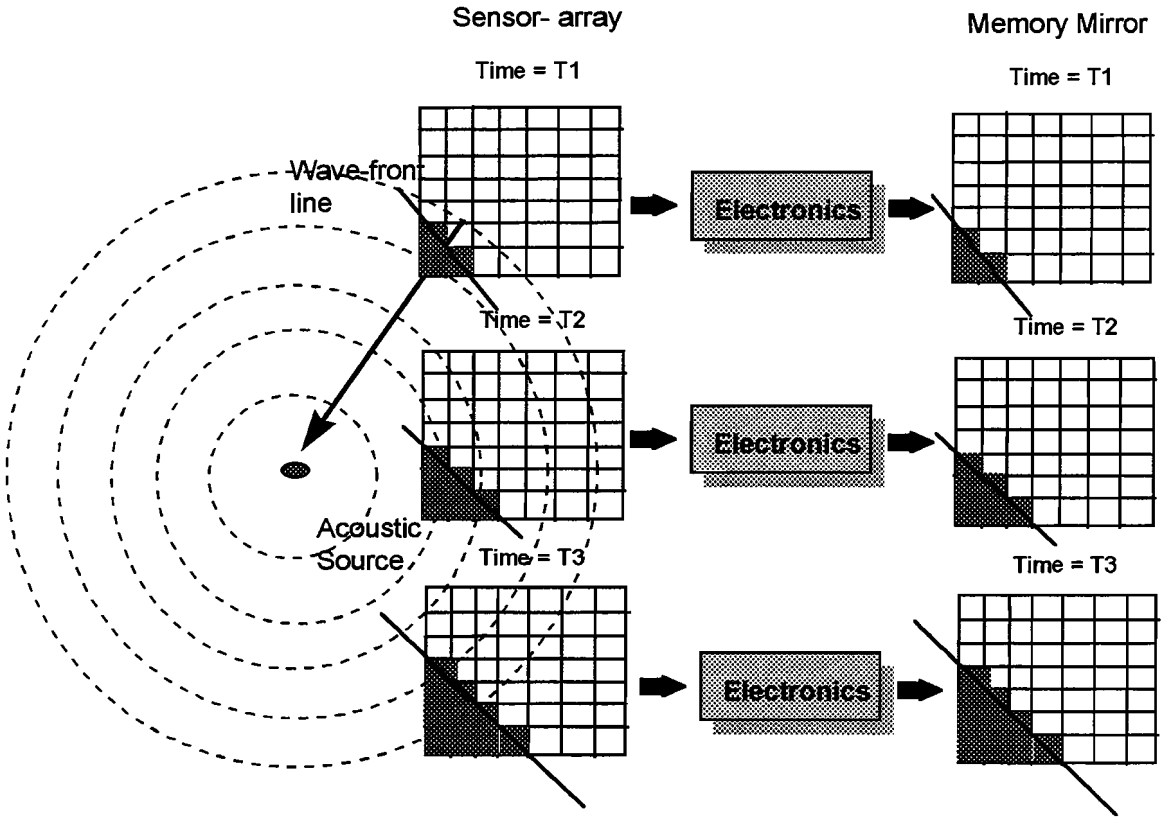

Figure 16. Schematic design showing the relationship between the sensor-array and the memory locations.

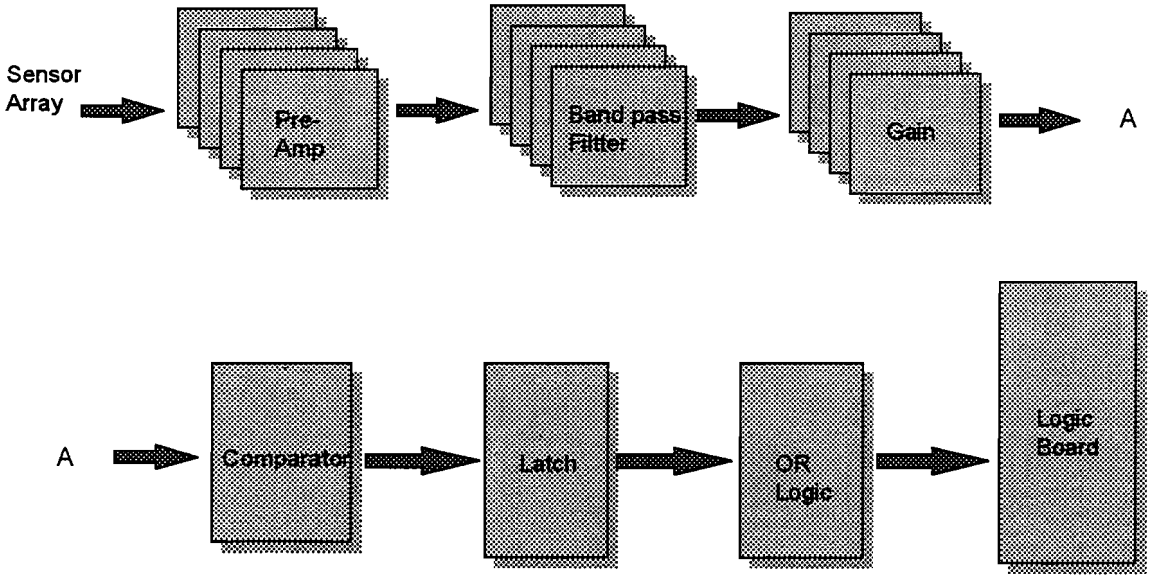

Figure 17. Schematic diagram of the logic used to register a high acoustic emission signal.

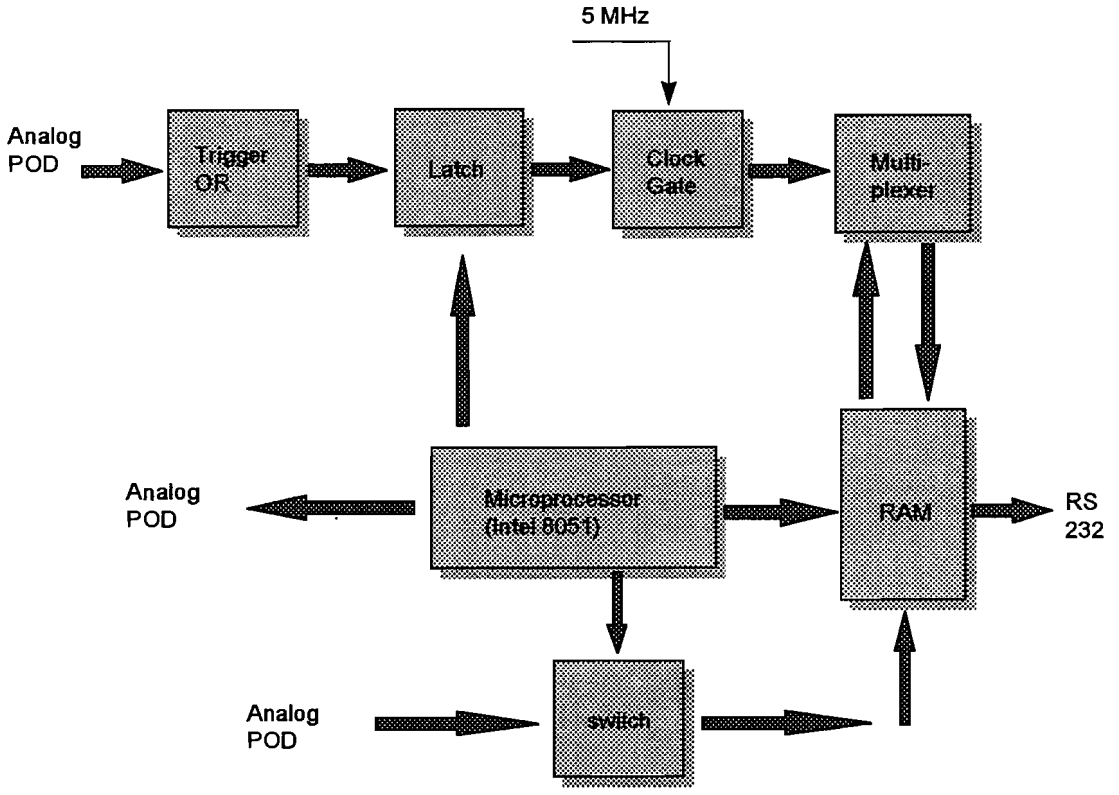

Figure 18. Schematic diagram of the digital logic circuit used to store an image of the sensor-array elements in RAM.

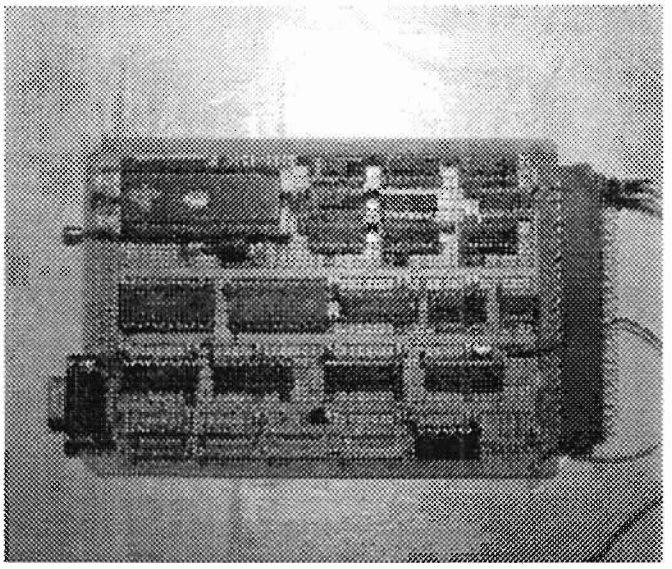

Figure 19. Photograph of the digital logic board.

4.1 Sensor Construction

The sensors were constructed from a PVDF polymer film. The sensors were fabricated from a process similar to that used to make printed circuit boards. The first step was to choose the number of elements in the sensor array. The total number of elements in the sensor array needed to be in multiples of 4 to be compatible with the sensor electronics. Therefore a 4 by 4 array was chosen since it is a good compromise between acceptable location accuracy and minimal numbers of elements.

The sensor array was fabricated using a process similar to that used for making printed circuit boards. The first step was to produce a CAD drawing of the sensor elements and this is shown in Figure 20. This CAD drawing represented the sensor pattern and was created using a commercial CAD package. A photo-resistance compound was sprayed on the sensor film and the sensor pattern, which acts as a mask, was placed over the photo-resist. The film was exposed to light and then soaked in a chemical bath to remove the exposed areas. A photograph of the finished sensor for the square array is shown in Figure 21. As shown in the figure leads have been attached to the sensor elements.

The sensor array was connected to the analog pod boards which were then connected to the logic board. A photograph of the finished sensor connected to the analog pods is shown in Figure 21. As shown in Figure 21 careful shielding was required for the leads since the sensor was very susceptible to RF pick-up. Further shielding was required for the analog and logic boards and each of the board was placed in a shielded boxes.

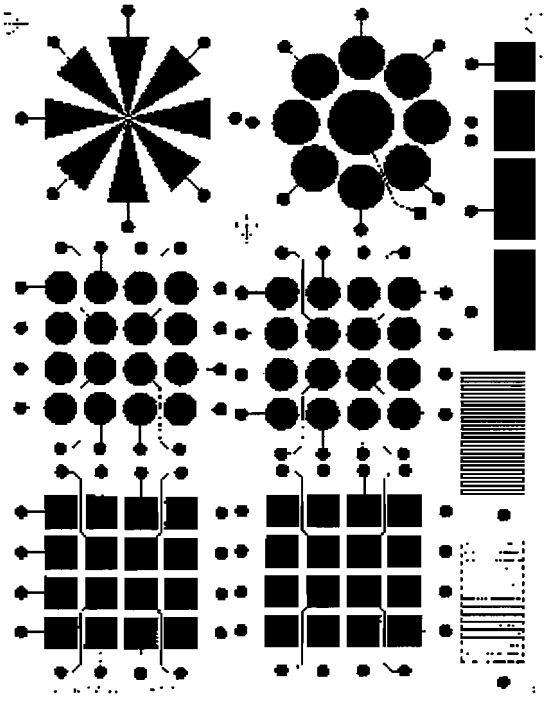

Figure 20. Photograph of the CAD sensor pattern used to make the sensor-arrays.

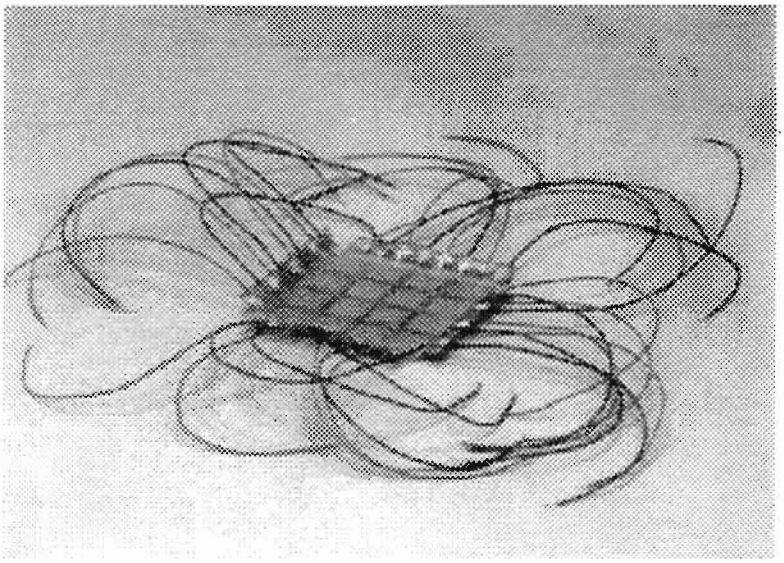

Figure 21. Photograph of the 4 by 4 sensor-array.

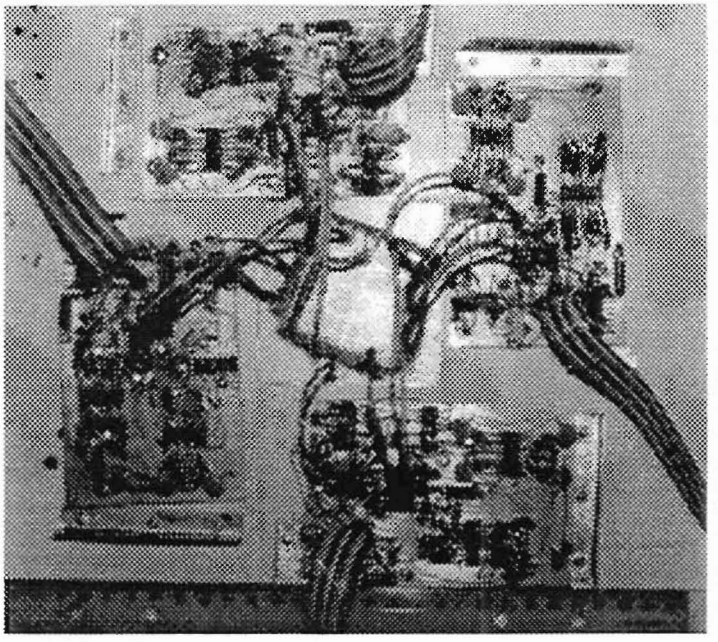

Figure 22. Photograph of the 4 by 4 sensor-array connected to the pre-amplifier boards.

4.0 Tests of Prototype Sensor Arrays

Tests were performed to test the sensor array. The test setup to test the sensor array is shown in Figure 23. As shown in Figure 23 the pulser was placed a distance of approximately 200 mms from the sensor array at successive angles of 0° and 45°

The output from the logic boards was sent via the RS-232 to the PC. The computer stored the data and a program was written to display successive images of the sensor array on the computer. Examples of the computer screen are shown in Figure 24. The time between frames was a function of the clock speed on the logic boards given in Figure 18 and for the tests performed here a 5 MHz clock was used which produced a time between frames of 200 nS.

The results from successive tests at 0° and 45° are now presented. The results from selected frames for the 0° tests are given in Figure 25. As shown in Figure 25 the array correctly predicts the wave-front direction. However as shown in the figure several of the elements did not trigger. This was due to the different sensitivities for the elements produced primarily by the difficulty of obtaining uniform contact sensitivity. Also shown in the Figure are the times after first sensor trigger.

The results from selected frames for the 45° tests are given in Figure 26. As shown in Figure 26 the array correctly identifies the wave direction.

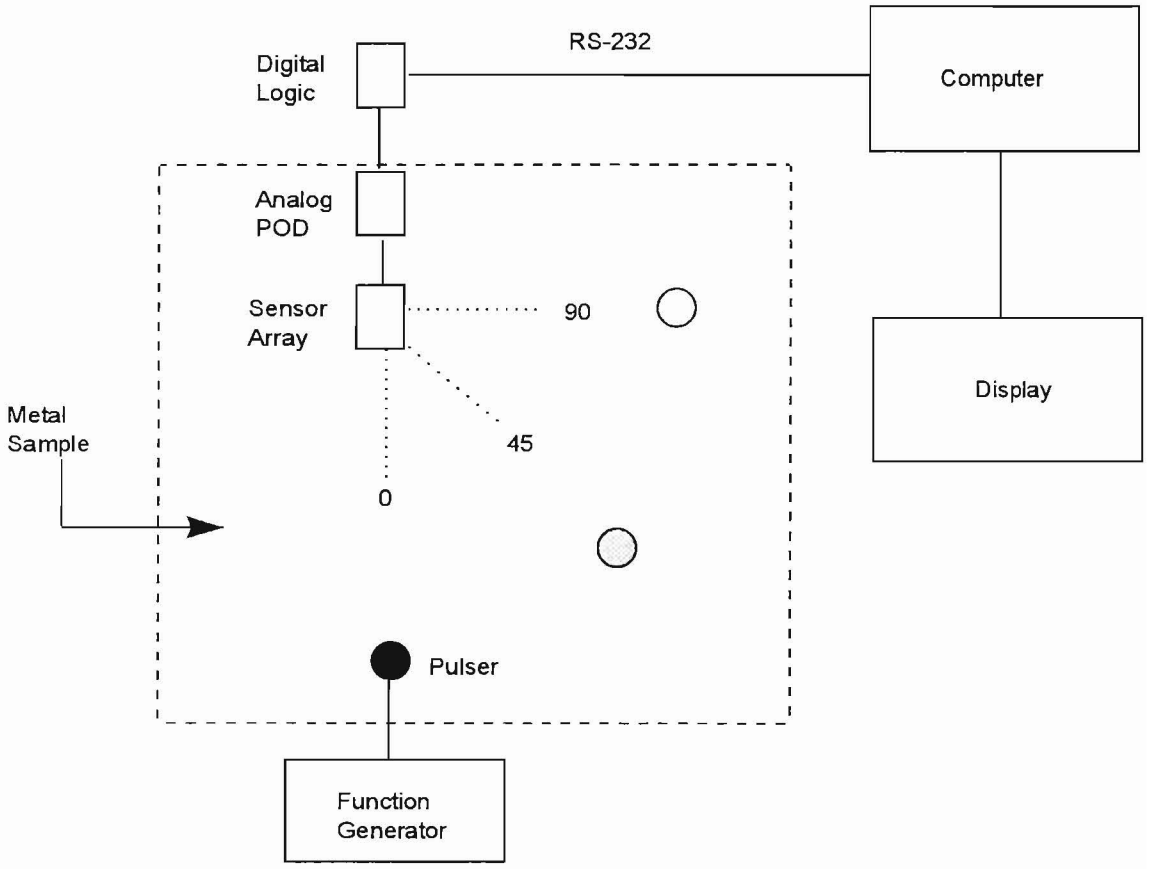

Figure 23. Test set-up used to perform tests on sensor-array

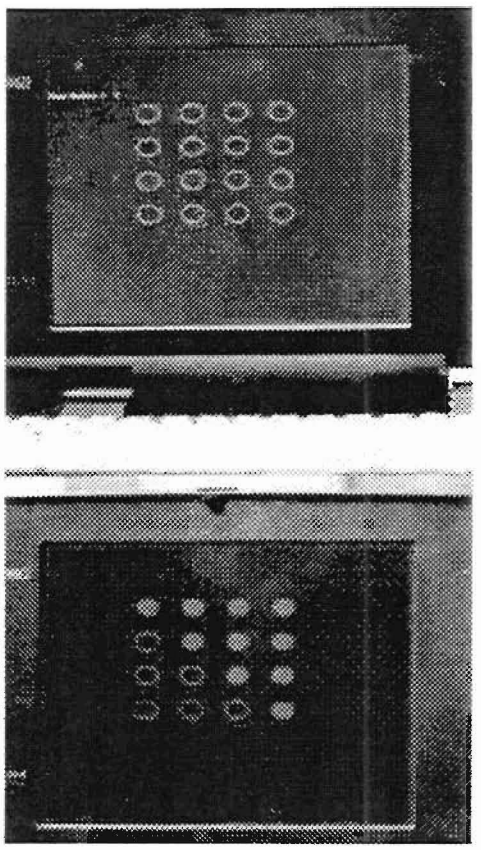

Figure 24. Photograph of the computer screen from the sensor array tests. Dark circles represent elements that have been triggered.

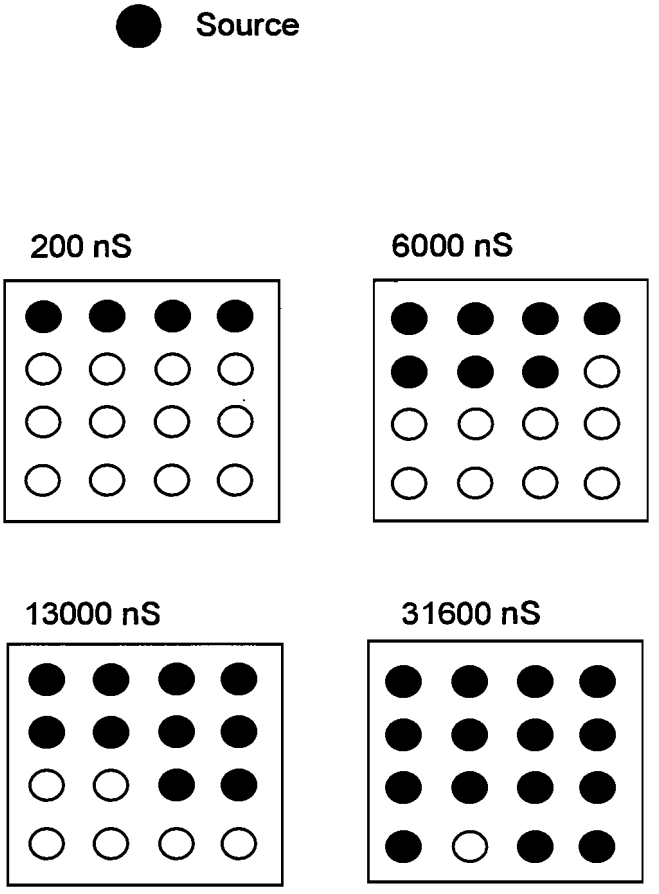

Figure 25. Results from the tests performed at 0°. The dark circles represent sensors that have been triggered.

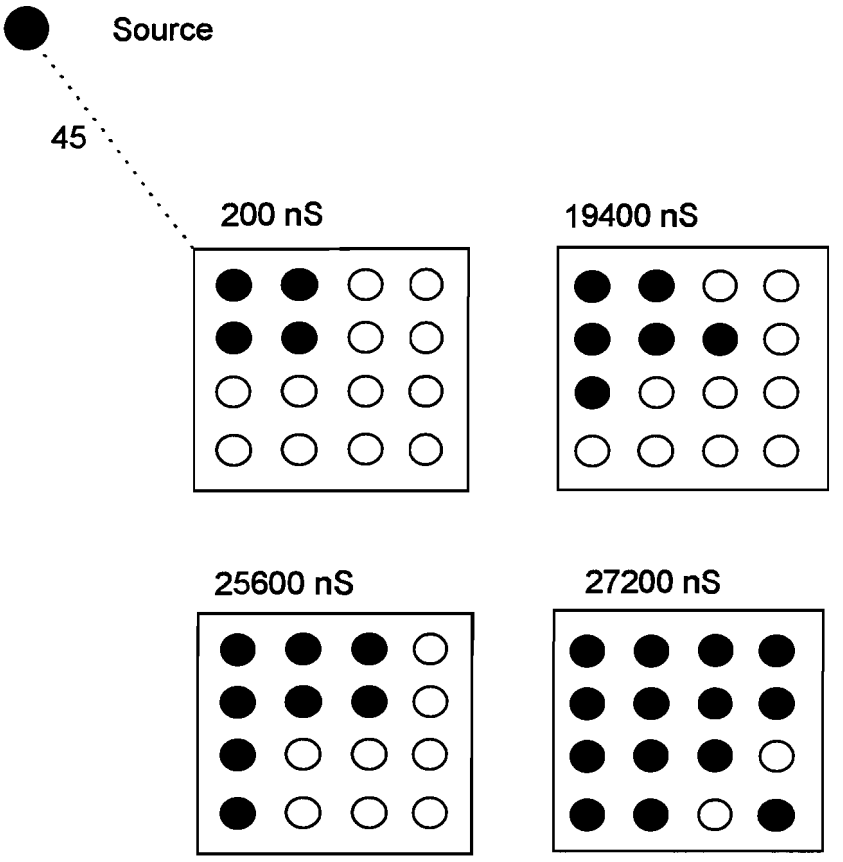

Figure 26. Results from the tests performed at 45°. The dark circles represent sensors that have been triggered.

5.0 Estimate of Technical Feasibility

The above results have clearly demonstrated the feasibility of using a sensor-array to locate acoustic emission sources. A prototype sensor-array was constructed and was shown to be capable of determining the location of the acoustic emission sources. Development of this array would have a revolutionary effect on acoustic emission inspection. For rail tank car inspection the sensor array approach would provide unambiguous evidence of cracks at critical locations. It would also greatly increase the reliability of the technique by distinguishing between noise from cracks and other sources of acoustic emission. The sensor array is not limited to rail tank cars, Table 8 lists some other applications where the sensor array could be used.

One of the major advantages of the sensor-array is that it is a "*virtual instrument*" since the output from the sensor is sent to a standard RS-232 connection and can be read by the computer with no other processing required. All of the data processing is performed by the sensor and digital logic. This is in contrast to conventional PZT sensors where a large amount of instrumentation is required to analyze the sensor output. In view of the significant difference between the sensor-array technology and conventional acoustic emission technology it may be appropriate to use other terminology to describe the technique. Suggested terms are source acoustics or acoustic tomography.

Table 8. Current acoustic emission inspection where sensor-arrays could be used.

Application	Advantage of sensor array
Rail tank car	Capable of locating cracks at critical locations
Bucket truck inspection	Capable of locating fiber breaks
Cylinder inspection	Capable of locating cracks in high pressure gas cylinders
Leak detection	Capable of accurately locating leaks
Fiberglass pressure vessels	Capable of locating sources of fiber damage

For the current rail tank car inspection the sensor-array approach could be used. This would require some modification to the AAR AE test procedure, which should not, in principle, be difficult provided the data are available to support the sensor-array concept. The current AAR test procedure does not utilize the concept of source location and does not use the sensor-arrays. It would be proposed to use the sensor-array as an addition to the current procedure. In particular the sensor array would be only used at locations such as the stub sill where identifying cracks is likely to have a major benefit.

In any case there are some practical problems that must be overcome before the sensor-array technology could be proposed to the AAR committee and these are (1) the need to reduce the size of the sensor array and (2) the need to obtain data to validate the technique. Each of these issues is now addressed in turn.

The key for successful development is to ensure that the footprint is small so that the sensor can be easily mounted on the rail tank car. A schematic diagram of the type of sensor that is envisaged is shown in Figure 27. As shown in Figure 27 the sensor will have a footprint of 25 mms and the digital logic will have a 75 mms footprint. To develop this sensor a number of issues must be addressed:

(1) Miniaturization of sensor array electronics
(2) Optimization of sensor-array size and mounting
(3) Optimization of control logic

The sensor-array with the associated electronics is shown in Figure 22. As shown in the figure, for the prototype constructed in this phase the pre-amplifier electronics were mounted on a brass board. A surface mount circuit board should be constructed to replace this electronics. This circuit board would greatly reduce the sensor size. This circuit board should be directly attached to the sensor-array using edge connectors, and should be mounted above the array. This design would also reduce noise since there will be no leads from the sensor-array as shown in Figure 22.

The sensor array size should also be reduced. The prototype sensor array has a footprint of 50 mms square and each element is 10 mms square. For the commercial sensor this size will be reduced to 25 mms square with an element size of 5 mms square. This should not present a major difficulty although the smaller sensor will be less sensitive since the sensitivity is proportional to the surface area. To compensate for this, extra gain will be added to the circuit.

Major enhancements are proposed for the digital logic. The current on-board RAM size in the prototype system is 2KB. Due to this limited storage the data must be sent to the host computer very frequently. By increasing the RAM size to 1 MB all of the data can be stored on-board which will greatly reduce the buffer writes. This is significant since it will also enable multiple sensors to be networked and controlled by a single computer.

The other major requirement for technical feasibility is demonstration of the technique for rail tank car inspection. The final sensor that is designed and fabricated should be tested on actual tank cars. These tests should be extensive. This will be a critical requirement for industry acceptance of the technique.

6.0 Acknowledgments

Cyltek, Inc would like to acknowledge the following organizations and personnel for there encouragement and support:

(1) Federal Railroad Administration of the Department of Transportation: (Mr. Pena and Ms. Hattery)
(2) Union Tank Car Company (Mr. DeLaFosse)

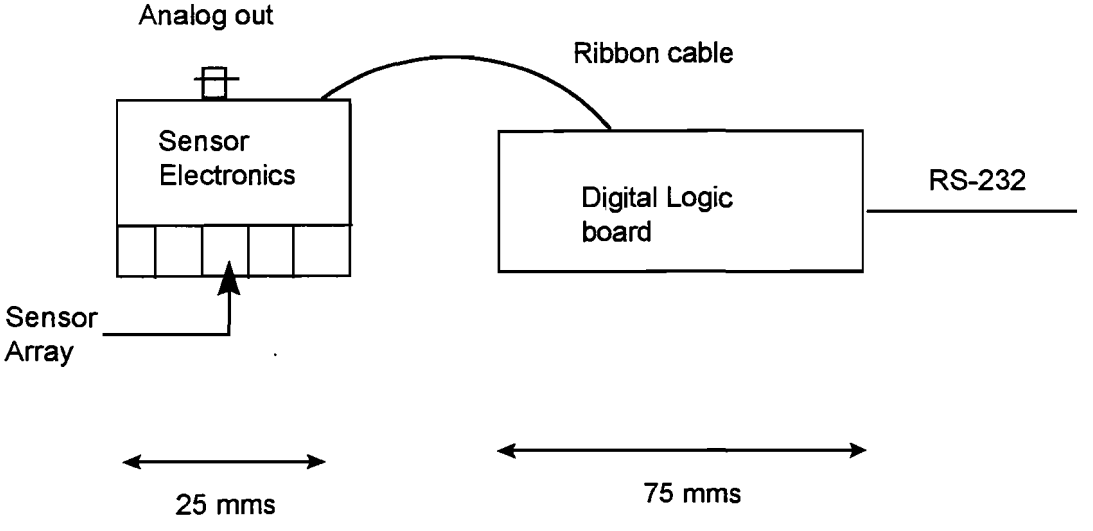

Figure 27. Schematic diagram of the improved sensor-array.